

Deep Reinforcement Learning for Unmanned Aerial Vehicle-Assisted Vehicular Networks

Ming Zhu*, Xiao-Yang Liu*, and Xiaodong Wang

Abstract—Unmanned aerial vehicles (UAVs) are envisioned to complement the 5G communication infrastructure in future smart cities. Hot spots easily appear in road intersections, where effective communication among vehicles is challenging. UAVs may serve as relays with the advantages of low price, easy deployment, line-of-sight links, and flexible mobility. In this paper, we study a UAV-assisted vehicular network where the UAV jointly adjusts its transmission power and bandwidth allocation under 3D flight to maximize the total throughput. First, we formulate a Markov Decision Process (MDP) problem by modeling the mobility of vehicles and the state transitions. Secondly, we solve the target problem using a deep reinforcement learning method, namely, the deep deterministic policy gradient, and propose three solutions with different control objectives. Thirdly, in a simplified model with small state and action spaces, we verify the optimality of proposed algorithms. Comparing with two baseline schemes, we demonstrate the effectiveness of proposed algorithms in a realistic model.

Index Terms—Unmanned aerial vehicle, vehicular networks, smart cities, Markov decision process, deep reinforcement learning, power control, bandwidth control.

I. INTRODUCTION

Intelligent transportation system [1] [2] [3] [4] is a key component of smart cities, which employs real-time data transmission for traffic monitoring, path planning, entertainment and advertisement [5]. High speed vehicular networks [6] emerge as a key component of intelligent transportation systems that provide cooperative communications to improve data transmission performance.

With the increasing number of vehicles, the current communication infrastructure may not satisfy data transmission requirements, especially when hot spots (e.g., road intersections) appear during rush hours. Unmanned aerial vehicles (UAVs) or drones [7] can complement the 4G/5G communication infrastructure, including vehicle-to-vehicle (V2V) communications, and vehicle-to-infrastructure (V2I) communications. Qualcomm has received a certification of authorization allowing for UAV testing below 400 feet [8]; Huawei will cooperate with China Mobile to build the first cellular test network for regional logistics UAVs [9].

*Contribute equally.

This work was supported by Leading Talents Program of Guangdong Province under grant 00201510, and the Shenzhen Peacock program under grant No. KQTD2015071715073798.

M. Zhu is with the Shenzhen Institutes of Advanced Technology, Chinese Academy of Sciences, Shenzhen 518055, China. E-mail: zhumingpassional@gmail.com.

X.-Y. Liu and X. Wang are with the Department of Electrical Engineering, Columbia University, New York, NY 10027, USA E-mail: {xiaoyang, wangx}@ee.columbia.edu.

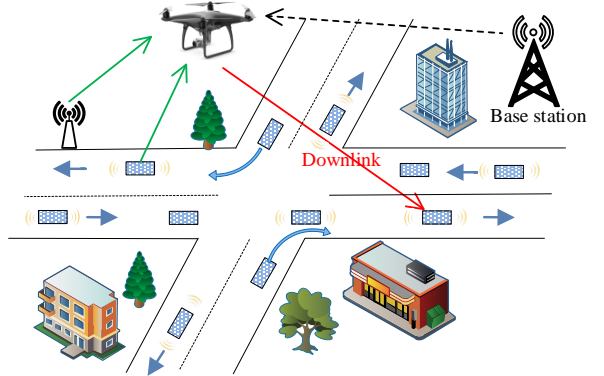


Fig. 1. The scenario of a UAV-assisted vehicular network.

A UAV-assisted vehicular network in Fig. 1 has several advantages. First, the path loss will be much lower since the UAV can move nearer to vehicles compared with stationary base stations. Secondly, the UAV is flexible in adjusting the transmission control [10] considering the mobility of vehicles. Thirdly, the quality of UAV-to-vehicle links is generally better than that of terrestrial links [11], since they are mostly line-of-sight (LoS).

Maximizing the total throughput of UAV-to-vehicle links has several challenges. First, the communication channels vary with the UAV's three-dimensional (3D) positions. Secondly, the joint adjustment of the UAV's 3D flight and transmission control (e.g., power control) cannot be solved directly using conventional optimization methods, especially when the environment is unknown. Thirdly, the channel conditions are hard to acquire, e.g., the path loss from the UAV to vehicles is closely related to the height/density of buildings and street width.

In this paper, we propose a deep reinforcement learning method to maximize the total throughput of UAV-to-vehicle communications, which jointly adjusts the UAV's 3D flight and transmission control learned by interacting with the environment. The main contributions of this paper can be summarized as follows: 1) We formulate the problem as a Markov decision process (MDP) problem to maximize the total throughput with the constraints of total transmission power and total bandwidth; 2) We apply a deep reinforcement learning method, the deep deterministic policy gradient (DDPG), to solve the problem. DDPG is suitable to solve MDP problems with continuous states and actions. We propose three solutions with different control objectives to jointly adjust the UAV's 3D

flight and transmission control; 3) We provide extensive simulation results to demonstrate the effectiveness of the proposed solutions compared with two baseline schemes, namely, Cycle and Greedy.

The remainder of the paper is organized as follows. Section II discusses related works. Section III presents system models and problem formulation. Solutions are proposed in Section IV. Section V presents the performance evaluation. Section VI concludes this paper.

II. RELATED WORKS

The dynamic control for the UAV-assisted vehicular networks includes flight control and transmission control. Flight control mainly includes the planning of flight path, time, and direction. Yang *et al.* [12] proposed a joint genetic algorithm and ant colony optimization method to obtain the best UAV flight paths to collect sensory data in wireless sensor networks. To further minimize the UAVs' travel duration under certain constraints (e.g., energy limitations, fairness, and collision), Garraffa *et al.* [13] proposed a two-dimensional (2D) path planning method based on a column generation approach. Liu *et al.* [14] proposed a deep reinforcement learning approach to control a group of UAVs by optimizing the flying directions and distances to achieve the best communication coverage in the long run with limited energy consumption.

The transmission control of UAVs mainly concerns resource allocations, e.g., access selection, transmission power and bandwidth allocation. Wang *et al.* [15] presented a power allocation strategy for UAVs considering communications, caching, and energy transfer. In a UAV-assisted communication network, Yan *et al.* [16] studied a UAV access selection and base station bandwidth allocation problem, where the interaction among UAVs and base stations was modeled as a Stackelberg game, and the uniqueness of a Nash equilibrium was obtained.

Joint control of both UAVs' flight and transmission has also been considered. Wu *et al.* [17] maximized the minimum achievable rates from a UAV to ground users by jointly optimizing the UAV's 2D trajectory and power allocation. Zeng *et al.* [18] proposed a convex optimization method to optimize the UAV's 2D trajectory to minimize its mission completion time while ensuring each ground terminal recovers the file with high probability when the UAV disseminates a common file to them. Zhang *et al.* [19] minimized the UAV mission completion time by optimizing its 2D trajectory with a constraint on the connectivity quality from base stations to a UAV. However, most existing research works neglected adjusting UAVs' height to obtain better quality of links by avoiding various obstructions or non-line-of-sight (NLoS) links.

[20] optimized the UAV's 3D flight and transmission control together; however, the 3D position optimization was converted to a 2D position optimization by the LoS link requirement. The existing deep reinforcement learning based method only handles UAVs' 2D flight and simple transmission control decisions. For example, Challita *et al.* [21] proposed a deep reinforcement learning based method for a cellular UAV network by optimizing the 2D path and cell association to

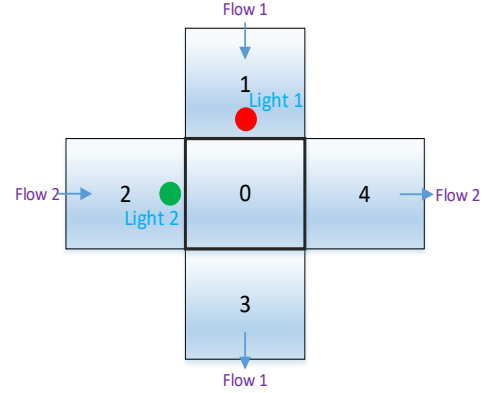


Fig. 2. A one-way-two-flow road intersection.

TABLE I
VARIABLES IN COMMUNICATION MODEL

$p^{i,\text{LoS}}, p^{i,\text{NLoS}}$	probabilities of LoS and NLoS links between the UAV and a vehicle in block i .
$h^{i,\text{LoS}}, h^{i,\text{NLoS}}$	channel power gain under LoS and NLoS links from the UAV to a vehicle in block i .
h^i	channel power gain from the UAV to a vehicle in block i .
ψ^i	SINR from the UAV to a vehicle in block i .
d_i, D_i	horizontal distance and Euclidean distance between the UAV and a vehicle in block i .
P, B	total transmission power and total bandwidth.
ρ^i, b^i	transmission power and bandwidth allocated for the vehicle(s) in block i .

achieve a tradeoff between maximizing energy efficiency and minimizing both wireless latency and the interference on the path. A similar scheme is applied to provide intelligent traffic light control [22].

In addition, most existing works assumed that the ground terminals are stationary; whereas in reality, some ground terminals move with certain patterns, e.g., vehicles move under the control of traffic lights. This work studies a UAV-assisted vehicular network where the UAV's 3D flight and transmission control can be jointly adjusted, considering the mobility of vehicles in a road intersection.

III. SYSTEM MODELS AND PROBLEM FORMULATION

In this section, we first describe the traffic model and communication model, and then formulate the target problem as a Markov decision process. The variables in the communication model are listed in Table I for easy reference.

A. Traffic Model

We start with a one-way-two-flow road intersection, as shown in Fig. 2, while a much more complicated scenario in Fig. 7 will be evaluated in Section V. Five blocks are numbered as 0, 1, 2, 3, and 4, where block 0 is the intersection. We assume that each block contains at most one vehicle, indicated by binary variables $n_0, \dots, n_4 \in \{0, 1\}$. There are two traffic flows in Fig. 2.

- “Flow 1”: 1 → 0 → 3;
- “Flow 2”: 2 → 0 → 4.

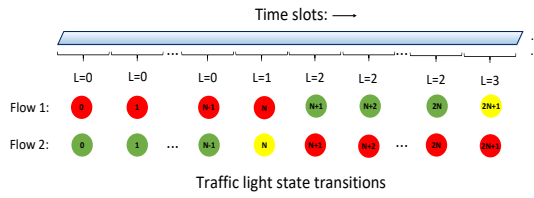


Fig. 3. Traffic light states along time.

The traffic light L has four configurations:

- $L=0$: red light for flow 1 and green light for flow 2;
- $L=1$: red light for flow 1 and yellow light for flow 2;
- $L=2$: green light for flow 1 and red light for flow 2;
- $L=3$: yellow light for flow 1 and red light for flow 2.

Time is partitioned into slots with equal duration. The duration of a green or red light occupies N time slots, and the duration of a yellow light occupies 1 time slot, which are shown in Fig. 3. We assume that each vehicle moves one block in a time slot if the traffic light is green.

B. Communication Model

We focus on the downlink communication (UAV-to-vehicle), since they are directly controlled by the UAV. There are two types of UAV-to-vehicle links, line-of-sight (LoS) and non-line-of-sight (NLoS). Let x and z denote the block (horizontal position) and height of the UAV respectively, where $x \in \{0, 1, 2, 3, 4\}$ corresponds to these five blocks in Fig. 2. Next, we describe the communication model, the channel power gain, the signal to interference and noise ratio (SINR), and the total throughput. First, the channel power gain h^i is formulated as [10] [23]

$$h^i = \begin{cases} h^{i,\text{LoS}}, & \text{with probability } p^{i,\text{LoS}}, \\ h^{i,\text{NLoS}}, & \text{with probability } p^{i,\text{NLoS}}. \end{cases} \quad (1)$$

where $p^{i,\text{LoS}}$ and $p^{i,\text{NLoS}}$ are probabilities of LoS and NLoS links between the UAV and a vehicle in block i , respectively, and $h^{i,\text{LoS}}$ and $h^{i,\text{NLoS}}$ are the channel power gain under LoS and NLoS links, respectively. $p^{i,\text{LoS}}$ and $p^{i,\text{NLoS}}$ are given by [24]

$$p^{i,\text{LoS}} = \frac{1}{1 + \alpha_1 \exp(-\alpha_2 (\frac{180}{\pi} \arctan \frac{z}{d_i} - \alpha_1))}, \quad (2)$$

$$p^{i,\text{NLoS}} = 1 - p^{i,\text{LoS}}, \quad i \in \{0, 1, 2, 3, 4\}, \quad (3)$$

where α_1 and α_2 are system parameters depending on the environment, such as the density/height of buildings/trees and the street width, and d_i is the horizontal distance. The angle $\frac{180}{\pi} \arctan \frac{z}{d_i}$ is measured in “degrees” with the range $0^\circ \sim 90^\circ$. $h^{i,\text{LoS}} = D_i^{-\beta_1}$ and $h^{i,\text{NLoS}} = \beta_2 D_i^{-\beta_1}$ [24], where D_i is the Euclidean distance between the UAV and a vehicle in block i , β_1 is the path loss exponent, and β_2 is an additional attenuation factor caused by NLoS connections.

Secondly, the SINR ψ_t^i in time slot t from the UAV to a vehicle in block i is characterized as [25]

$$\psi_t^i = \frac{\rho_t^i h_t^i}{b_t^i \sigma^2}, \quad i \in \{0, 1, 2, 3, 4\}, \quad (4)$$

where ρ_t^i and b_t^i are the allocated transmission power and bandwidth for the vehicle(s) in block i in time slot t , respectively, and σ^2 is the additive white Gaussian noise (AWGN) power spectrum density, and h_t^i is formulated by (1). We assume that the UAV uses orthogonal frequency division multiple access (OFDMA) systems [26]; therefore, there is no interference among these channels.

Thirdly, the total throughput (reward) of UAV-to-vehicle links is formulated as [27]

$$\sum_{i \in \{0, 1, 2, 3, 4\}} b_t^i \log(1 + \psi_t^i) = \sum_{i \in \{0, 1, 2, 3, 4\}} b_t^i \log\left(1 + \frac{\rho_t^i h_t^i}{b_t^i \sigma^2}\right). \quad (5)$$

C. MDP Formulation

The UAV aims to maximize the total throughput with the constraints of total transmission power and bandwidth:

$$\sum_{i \in \{0, 1, 2, 3, 4\}} \rho_t^i \leq P, \quad \sum_{i \in \{0, 1, 2, 3, 4\}} b_t^i \leq B,$$

where P is the total transmission power, and B is the total bandwidth, and $\rho_t^i \in [0, P]$, $b_t^i \in [0, B]$. We assume that there are totally κ channels.

The target UAV-assisted communication problem is a Markov decision process (MDP) problem. On the one hand, from (1) we know that the channel power chain of UAV-to-vehicle links follows a stochastic process. On the other hand, the arrival of vehicles follows a stochastic process under the control of the traffic light.

Under the MDP framework, the state space \mathcal{S} , action space \mathcal{A} , reward r , policy π , and state transition probability $p(s_t, a_t, s_{t+1})$ of our problem are defined as follows.

- State $\mathcal{S} = (L, x, z, n, H)$, where L is the traffic light state, (x, z) is the UAV’s 3D position with $x \in \{0, 1, 2, 3, 4\}$ being the block and $z \in \{z^0, z^1, \dots, z^K\}$ ($z^0 < z^1 < \dots < z^K$) being the height, $n = (n^0, \dots, n^4)$ is the number of vehicles in those five blocks, and $H = (H^0, \dots, H^4)$ is the channel state from the UAV to each block with $H^i \in \{\text{NLoS, LoS}\}$. The block x is the location projected from UAV’s 3D position to the road networks. The UAV’s height is discretized to K equal distance.
- Action $\mathcal{A} = (\mathbf{f}, \rho, b)$ denotes the action set. \mathbf{f} is the UAV’s 3D flight, which includes horizontal and vertical movement. $\rho = (\rho^0, \dots, \rho^4)$ and $b = (b^0, \dots, b^4)$ are the transmission power and bandwidth allocation policies for those five blocks, respectively. At the end of time slot t , the UAV moves to a new 3D position according to action \mathbf{f} , and over time slot t , the transmission power and bandwidth are ρ and b , respectively.
- Reward $r(s_t, a_t) = \sum_{i \in \{0, 1, 2, 3, 4\}} b_t^i \log\left(1 + \frac{\rho_t^i h_t^i}{b_t^i \sigma^2}\right)$ is the total throughput (according to (4) and (5)) after a transition from state s_t to s_{t+1} taking action a_t . Note that the total throughput over the t -th time slot is measured at the state $s_t = (L_t, x_t, z_t, n_t, H_t)$.
- Policy π is the strategy for the UAV, which maps states to a probability distribution over the actions $\pi : \mathcal{S} \rightarrow \mathcal{P}(\mathcal{A})$, where $\mathcal{P}(\cdot)$ denotes probability distribution. In time slot t ,

the UAV's state is $s_t = (L_t, x_t, z_t, n_t, H_t)$, and its policy π_t outputs the probability distribution over the action a_t . We see that the policy indicates the action preference of the UAV.

- State transition probability $p(s_t, a_t, s_{t+1})$ is the probability of the UAV entering the new state s_{t+1} , after taking the action a_t at the current state s_t . At the current state $s_t = (L_t, x_t, z_t, n_t, H_t)$, after taking the flight and transmission control $a_t = (\mathbf{f}, \rho, b)$, the UAV moves to the new 3D position (x_{t+1}, z_{t+1}) , and the channel state changes to H_{t+1} , with the traffic light changes to L_{t+1} and the number of vehicles in each block changes to n_{t+1} .

Next, we discuss the MDP in three aspects: the state transitions of the traffic light and the number of vehicles in each block, the state transitions of UAV's 3D position, and the state transition probability.

The state transitions of the traffic light along time are shown in Fig. 3. Let λ_1 and λ_2 be the probability of the arrivals of new vehicles in flow 1 and 2, and $\{n_t^i\}_{i \in \{0,1,2,3,4\}}$ be the number of vehicles in each block in time slot t . Let \mathbb{I} be an indicator function. The state transition for the number of vehicles in each block is

$$n_{t+1}^0 = \begin{cases} n_t^2, & \text{if } L_t = 0, \\ n_t^1, & \text{if } L_t = 2, \\ 0, & \text{otherwise.} \end{cases} \quad (6)$$

$$n_{t+1}^1 = \begin{cases} 1, & \text{with probability } \lambda_1, \\ n_t^1 \mathbb{I}_{\{L_t \neq 2\}}, & \text{with probability } (1 - \lambda_1), \end{cases} \quad (7)$$

$$n_{t+1}^2 = \begin{cases} 1, & \text{with probability } \lambda_2, \\ n_t^2 \mathbb{I}_{\{L_t \neq 0\}}, & \text{with probability } (1 - \lambda_2), \end{cases} \quad (8)$$

$$n_{t+1}^3 = \begin{cases} n_t^0, & \text{if } L_t = 2, 3, \\ 0, & \text{otherwise,} \end{cases} \quad (9)$$

$$n_{t+1}^4 = \begin{cases} n_t^0, & \text{if } L_t = 0, 1, \\ 0, & \text{otherwise.} \end{cases} \quad (10)$$

The state transitions of UAV's 3D position include block transitions and height transitions. We assume that in time slot t the UAV's block x_t and height z_t is 1 and z^k respectively, where $k \in \{0, 1, \dots, K\}$. The UAV's vertical flight action in time slot t is denoted by an integer a_t^v , which may be negative, and its height state transition is

$$z_{t+1} = z_t + \epsilon a_t^v, \quad (11)$$

where ϵ is the height interval. If the UAV's height is fixed, the corresponding position state transition diagram is shown in Fig. 4, where $\{S_i\}_{i \in \{0,1,2,3,4\}}$ denotes the block of the UAV: 0 denotes staying in the current block; $\{1, 2, 3, 4\}$ denotes a movement from block 0 to the other blocks (1, 2, 3, and 4); 5 denotes an anticlockwise movement; 6 denotes a movement to block 0 from the other blocks; 7 denotes a clockwise movement.

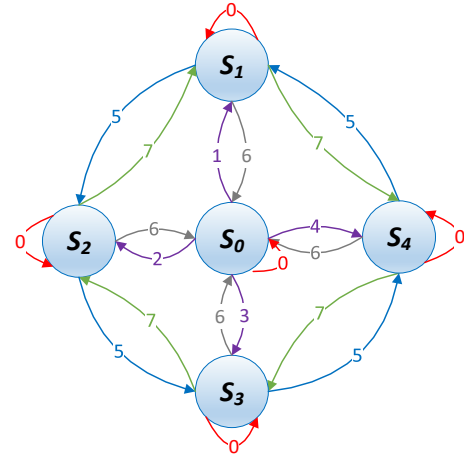


Fig. 4. The state transition diagram when the UAV's height is fixed.

For the state transition probability $p(s_t, a_t, s_{t+1})$, firstly, we discuss the channel state of UAV-to-vehicle links, which is a stochastic process. The UAV's flight in time slot t is $\mathbf{f}_t = (5, 0)$, where 5 denotes the UAV's horizontal anticlockwise movement in Fig. 4 and 0 denotes the UAV's vertical movement. The state transition probability of channel state for the vehicle in block 1 is

$$p(x_t = 1, z_t = z^k, \mathbf{f}_t = (5, 0), H_{t+1}^1 = \text{LoS}) = p^{1, \text{LoS}}, \quad (12)$$

$$p(x_t = 1, z_t = z^k, \mathbf{f}_t = (5, 0), H_{t+1}^1 = \text{NLoS}) = p^{1, \text{NLoS}}. \quad (13)$$

Here, the transmission power and bandwidth allocations do not affect the channel state, therefore, neither of both is not shown.

Secondly, we discuss the state transition probability for the number of vehicles, which is also a stochastic process. The traffic light state L and the number of vehicles n in each block are independent with the state, and thus neither of both is not presented. We assume that in time slot t the traffic light state is $L_t = 2$, and the number of vehicles in block 1 is $n_t^1 = 1$. The state transition probability for the number of vehicles in block 1 is

$$p(n_t^1 = 1, L_t = 2, n_{t+1}^1 = 1) = \lambda_1, \quad (14)$$

$$p(n_t^1 = 1, L_t = 2, n_{t+1}^1 = 0) = 1 - \lambda_1. \quad (15)$$

Here, the UAV's actions and states do not affect the number of vehicles of all blocks, thus, they are not shown.

IV. PROPOSED SOLUTIONS

In this section, we first present an overview of reinforcement learning, then introduce the deep deterministic policy gradient algorithm, and then propose three solutions with different control objectives, and finally discuss how to transfer DDPG output action to the UAV's real action in proposed solutions.

A. Reinforcement Learning

RL with the essence of exploration and exploitation aims to maximize the expected return J from a start distribution by interacting with the environment E . The objective function



Fig. 5. Framework of the DDPG algorithm.

with the physical meanings of “expected rewards” can be $V(s_t)$ value for a state s_t , or $Q(s_t, a_t)$ value for a state-action pair (s_t, a_t) . For small state space, value iteration and policy gradient iteration are two standard algorithms. In our problem, RL helps the UAV learn to maximize the total throughput over a number of time slots in complicated scenarios without knowing the real-time traffic and communication environments. Then, the UAV applies the best policy to serve the vehicles, including the 3D flight and transmission control.

An RL problem can be described as a standard MDP. The return from a state is defined as the sum of discounted future reward $\sum_{i=t}^{T'} \gamma^{i-t} r(s_i, a_i)$, where T' is the total number of time slots, and $\gamma \in (0, 1)$ is a discount factor that diminishes the future reward and ensures that the sum of an infinite number of rewards is still finite. $Q(s_t, a_t)$ value represents the expected return after taking action a_t in state s_t under policy π :

$$Q^\pi(s_t, a_t) = \mathbb{E}_{r_{i \geq t}, s_{i \geq t} \sim E, a_{i \geq t} \sim \pi} \left[\sum_{i=t}^T \gamma^{i-t} r(s_i, a_i) | s_t, a_t \right],$$

where E is the environment. The aim of RL is to learn a policy

which maximizes the expected return from a start distribution:

$$J = \mathbb{E}_{r_i, s_i \sim E, a_i \sim \pi} \sum_{i=1}^T \gamma^{i-1} r(s_i, a_i). \quad (16)$$

Many reinforcement learning approaches use the recursive relationship known as Bellman equation for action-value function [28]:

$$Q^\pi(s_t, a_t) = \mathbb{E}_{r_t, s_{t+1} \sim E} [r(s_t, a_t) + \gamma \mathbb{E}_{a_{t+1} \sim \pi} Q^\pi(s_{t+1}, a_{t+1})], \quad (17)$$

and the optimal action-value is

$$Q^{\pi^*}(s_t, a_t) = \max_{\pi} \mathbb{E}_{r_t, s_{t+1} \sim E} Q^\pi(s_t, a_t), \quad (18)$$

where π^* is the optimal policy.

If the target policy is deterministic, a policy function $\mu : \mathcal{S} \rightarrow \mathcal{A}$ is introduced and the inner expectation of (17) can be removed:

$$Q^\mu(s_t, a_t) = \mathbb{E}_{r_t, s_{t+1} \sim E} [r(s_t, a_t) + \gamma Q^\mu(s_{t+1}, \mu(s_{t+1}))]. \quad (19)$$

Note that $Q^\mu(s_t, a_t)$ only depends on the environment E . Therefore, it is possible to learn Q^μ off-policy using transitions

which are generated from a different stochastic behavior policy β .

Q-learning [29] uses a greedy policy to get a new action $\mu(s_t) = \arg \max_{a_t} Q(s_t, a_t)$. We consider function approximators parameterized by θ^Q , which we optimize by the loss function:

$$\text{Loss}(\theta^Q) = \mathbb{E}_{s_t \sim \rho^\beta, a_t \sim \beta, r_t \sim E} [(y_i - Q(s_i, a_i | \theta^Q))^2], \quad (20)$$

where ρ^β is the state visitation distribution on the policy β , and

$$y_i = r_i + \gamma Q(s_{i+1}, \mu(s_{i+1} | \theta^\mu) | \theta^Q).$$

B. Deep Deterministic Policy Gradient

In our problem, some communication coefficients, e.g., α_1 , α_2 , β_1 , and β_2 , are unknown, since they are determined by the height/density of buildings and street width, the weather, and the UAV's 3D position, etc. Moreover, it takes too much labor and time to measure them. However, we can use neural networks to estimate them by the received reward. Therefore, we use deep RL instead of classical RL to solve our problem.

DDPG [30] uses deep neural networks to approximate both action policy and Q-value, exploiting the powerful skills introduced in AlphaGo zero [31] and Atari game playing [32]. Therefore, DDPG is much more efficient and performs better in a high dimensional task than the stochastic policy gradient [33] [22].

The actor-critic approach can solve the MDP with continuous action space: the actor approximates the action policy, and the critic approximates the Q-value.

The actor has two neural networks: the online policy network μ (parameter: θ^μ) with state s as input and action $\mu(s)$ as output and the target policy network μ' (parameter: $\theta^{\mu'}$) with θ^μ as input and action $\mu'(s)$ as output. The online policy network μ is updated following the chain rule for the expected return J in (16) from the start distribution with respect to the actor's parameters θ^μ :

$$\begin{aligned} \nabla_{\theta^\mu} J &= \mathbb{E}_{s_t \sim \rho^\beta} [\nabla_{\theta^\mu} Q(s, a | \theta^Q) |_{s=s_t, a=\mu(s_t | \theta^\mu)}] \\ &= \mathbb{E}_{s_t \sim \rho^\beta} [\nabla_a Q(s, a | \theta^Q) |_{s=s_t, a=\mu(s_t)} \nabla_{\theta^\mu} \mu(s | \theta^\mu) |_{s=s_t}]. \end{aligned} \quad (21)$$

The target policy network μ' is updated by slowly tracking the online policy network μ : $\theta^{\mu'} \leftarrow \tau \theta^\mu + (1 - \tau) \theta^{\mu'}$, where $\tau \ll 1$ is a low learning rate.

The critic also has two neural networks: the online Q-network Q (parameter: θ^Q) with a state-action pair (s, a) as input and Q-value $Q(s, a)$ as output and the target Q-network Q' (parameter: $\theta^{Q'}$) with θ^Q as input and Q-value $Q'(s, a)$ as output. It helps to evaluate the actions of the actor. The online Q-network (i.e., the evaluation of the UAV's actions) is updated by minimizing the loss function:

$$\nabla_{\theta^Q} \text{Loss}(\theta^Q) = \nabla_{\theta^Q} \left[\frac{1}{M} \sum_{i=1}^M (y_i - Q(s_i, a_i | \theta^Q))^2 \right], \quad (22)$$

where $\text{Loss}(\theta^Q)$ is given in (20). The target Q-network Q' is updated by slowly tracking the online Q-network Q : $\theta^{Q'} \leftarrow \tau \theta^Q + (1 - \tau) \theta^{Q'}$.

DDPG uses three skills to guarantee the UAV's communication performance and stability: experience replay buffer, learning rate, and exploration noise.

Experience replay buffer R_b in DDPG stores transitions that will be used for model update. Note that there are correlations between the UAV's consecutive transitions, leading to extremely slow convergence. DDPG stores each transition (s_t, a_t, r_t, s_{t+1}) in R_b , and then uniformly samples a mini-batch of M transitions, and executes stochastic gradient decent (SGD) [34] to update network weights for the critic network $Q(s, a)$. "Experience replay buffer" has two advantages: 1) enabling the stochastic gradient decent method; 2) and removing the correlations between consecutive transitions.

Learning rate $\tau \ll 1$ is introduced to soft update the target policy network μ' and the target Q-network Q' , which makes them more stable. They are updated according to μ and Q . This process makes the total throughput of the UAV-to-vehicle links more stable in the scenario of time-varying vehicle flows.

Exploration noise \mathcal{N}_t is added to the target policy to get a new action, i.e., $\tilde{a}_t = \mu'(s_t | \theta^{\mu'}) + \mathcal{N}_t$. Generally, the output of a neural network is $[-1, 1]$, and the noise is assumed to follow a standard normal distribution (a mean of 0 and a standard deviation of 1). It solves the tradeoff between exploration and exploitation, and the exploration is independently from the learning process. This ensures that the UAV has a certain probability of exploring other actions besides the one predicted by the current policy, and avoid that the UAV is trapped in a local optimum.

C. Deep Reinforcement Learning-based Solutions

We propose solutions using DDPG since it is able to learn continuous states/actions such as transmission power allocation. We know that state variable "traffic light state L " and action variable "the UAV's flight" are discrete. However, other state variables and action variables are continuous. In our problem, the UAV does not know the exact communication coefficients; however, through a series of trials, the total throughput function (5) can be approximated. Therefore, we choose DDPG to solve our problem.

The framework of DDPG is shown in Fig. 5. Adam optimizer [35] [36] is a computationally efficient method for stochastic optimization with little memory requirements, and is widely used in deep learning to update parameters. The agent receives the reward r_t and new state s_{t+1} from the environment after taking action a_t in state s_t , and then the state transition is stored in the experience replay buffer R_b . A mini-batch of M transitions are sampled from R_b to calculate the actor's policy by the chain rule as described above. The exploration noise \mathcal{N}_t is added to the target policy μ' to get an action of the UAV.

Despite the UAV's 3D flight control, the UAV has two communication controls, power and bandwidth. We assume the UAV can either choose power or bandwidth control, and then we propose three algorithms:

- **Power Control:** the UAV adjusts its 3D flight and the transmission power allocation using the actor network, and the bandwidth are equally allocated to each vehicle in each time slot.

Algorithm 1: DDPG-based algorithms: Power Control, Band Control, and Joint Control

Input: the number of episodes η , the number of timesteps T in an episode, the mini-batch size M , the learning rate τ ;

- 1: Initialize all states, including the traffic light state L , the UAV's 3D position (x, z) , the number of vehicles n and and the channel power gain h in all blocks, and then set the dimension of states;
- 2: Set the dimension of the UAV's actions in Power Control, Band Control, or Joint Control by (27);
- 3: Randomly initialize critic's online Q-network parameters θ^Q and actor's online policy network parameters θ^μ , and then initialize the critic's target Q-network parameters $\theta^{Q'} \leftarrow \theta^Q$ and actor's target policy network parameters $\theta^{\mu'} \leftarrow \theta^\mu$;
- 4: Initialize the UAV's experience replay buffer R_b ;
- 5: **for** episode $k = 1$ to η
- 6: Initialize a random process (a standard normal distribution) \mathcal{N} for the UAV's action exploration;
- 7: Observe the initial state s_1 ;
- 8: **for** $t = 1$ to T
- 9: Select the UAV's action $a_t = \mu'(s_t | \theta^{\mu'}) + \mathcal{N}_t$ according to the current policy and exploration noise \mathcal{N}_t ;
- 10: **if** Power Control
- 11: Add the equal bandwidth allocation policy $\{\bar{b}_t^i\}_{i=0}^4 = \{n_t^i\}_{i=0}^4$ as part of the UAV's action;
- 12: **if** Band Control
- 13: Add the equal transmission power allocation policy $\{\bar{p}_t^i\}_{i=0}^4 = \{n_t^i\}_{i=0}^4$ as part of the UAV's action;
- 14: Determine the scope of the UAV's horizontal flight, vertical flight, power allocation, and bandwidth allocation based on a_t , $\{\bar{b}_t^i\}_{i=0}^4$ (if Power Control), and $\{\bar{p}_t^i\}_{i=0}^4$ (if Band Control);
- 15: Obtain the UAV's real horizontal flight action a_t^h , vertical flight action a_t^v , power allocation $\{p_t^i\}_{i=0}^4$, and bandwidth allocation $\{b_t^i\}_{i=0}^4$ by (23), (24), (25) and (26), respectively. // Transfer the action a_t , $\{\bar{b}_t^i\}_{i=0}^4$ (if Power Control), and $\{\bar{p}_t^i\}_{i=0}^4$ (if Band Control) to the UAV's real actions;
- 16: Execute four type of actions a_t^h , a_t^v , $\{p_t^i\}_{i=0}^4$, and $\{b_t^i\}_{i=0}^4$, and receive reward r_t , and observe new state s_{t+1} from the environment;
- 17: Store transition (s_t, a_t, r_t, s_{t+1}) in the UAV's experience replay buffer R_b ;
- 18: Sample a random mini-batch of M transitions $\{s_i, a_i, r_i, s_{i+1}\}_{i=1}^M$ from the UAV's experience replay buffer R_b ;
- 19: Set $y_i = r_i + \gamma Q'(s_{i+1}, \mu'(s_{i+1} | \theta^{\mu'}) | \theta^{Q'})$;
- 20: Update the critic's online Q-network (i.e., the evaluation of the UAV's actions) by minimizing the loss function: $\nabla_{\theta^Q} \text{Loss}(\theta^Q) = \nabla_{\theta^Q} [\frac{1}{M} \sum_{i=1}^M (y_i - Q(s_i, a_i | \theta^Q))^2]$, where $\text{Loss}(\theta^Q)$ is given in (20);
- 21: Update the actor's online policy network (i.e., the UAV's policy) using the policy gradient by the chain rule: $\nabla_{\theta^\mu} J \approx \frac{1}{M} \sum_{i=1}^M \nabla_a Q(s, a | \theta^Q) |_{s=s_i, a=\mu(s_i)} \nabla_{\theta^\mu} \mu(s | \theta^\mu) |_{s=s_i}$;
- 22: Update the critic's target Q-network Q' and actor's target policy network μ' to make the UAV's policy and the evaluation of the UAV's actions more stable: $\theta^{Q'} \leftarrow \tau \theta^Q + (1 - \tau) \theta^{Q'}$, $\theta^{\mu'} \leftarrow \tau \theta^\mu + (1 - \tau) \theta^{\mu'}$;

- Band Control: the UAV adjusts its 3D flight and bandwidth allocation using the actor network, and the transmission power is equally allocated to each vehicle in each time slot.
- Joint Control: the UAV adjusts its 3D flight, the transmission power and bandwidth allocation using the actor network.

The DDPG-based algorithms are given in **Algorithm 1**. We describe the algorithm into three parts: initializations, the main process of DDPG, and the difference of the action structure in three algorithms. Finally, we describe the settings for the DDPG action space.

First, we describe the initializations in lines 1 ~ 4. In line 1, all states are initialized and the the dimension of states is obtained: the traffic light L is initialized as 0, the UAV's initial 3D position is the intersection block with a predefined height, and the number of vehicles n in all blocks is 0, and the channel power gain h as that obtained based on LoS links. Line 2 sets the dimension of the UAV's actions in Power Control, Band Control, and Joint Control, which is described in detail in the next subsection. Line 3 initializes the parameters of the critic and actor. Line 4 initializes the experience replay buffer R_b .

Secondly, we present the main process of DDPG. Line 6 initializes a random process for action exploration. Line 7 receives an initial state s_1 . Line 9 selects an action \tilde{a}_t according to the current policy and exploration noise. Lines 10 ~ 11 add the equal bandwidth allocation policy $\{\bar{b}_t^j\}_{j=0}^4 = \{\bar{n}_t^j\}_{j=0}^4$ in Power Control. Lines 12 ~ 13 add the equal power allocation policy $\{\bar{p}_t^j\}_{j=0}^4 = \{\bar{n}_t^j\}_{j=0}^4$ in Band Control. Line 14 determines the scope of the UAV's horizontal flight, vertical flight, power allocation, and bandwidth allocation based on a_t , added actions in Power Control and Band Control. Line 15 obtains the UAV's horizontal flight action, vertical flight action, power allocation, and bandwidth by (23), (24), (25) and (26), respectively. Line 16 executes four type of actions a_t^h , a_t^v , $\{p_t^i\}_{i=0}^4$, and $\{b_t^i\}_{i=0}^4$, and then the reward and all states will be updated. Line 17 stores the UAV's experience into R_b . In line 18, a random mini-batch will be sampled uniformly. Line 19 sets the value of y_i . Line 20 updates the critic's online Q-network, and line 21 updates the actor's online policy network. Lines 22 updates the critic's target Q-network, and the actor's target policy network.

Thirdly, we discuss the difference of the action structure in three algorithms presented in lines 10 ~ 14. In Power

Control (lines 10 ~ 11), the action a_t , and the equal bandwidth allocation policy $\{\bar{b}_t^i\}_{i=0}^4$ in 5 blocks are combined as a new action. In Band Control (lines 12 ~ 13), the action a_t , and the equal transmission power policy $\{\bar{p}_t^i\}_{i=0}^4$ in 5 blocks are combined as a new action. In Joint Control, no policy is added since DDPG outputs all policies of the UAV, i.e., UAV's horizontal and vertical flight, power allocation, and bandwidth allocation. Line 14 determines the scope of the UAVs four type of actions. In Power Control, the bandwidth allocation is exactly the added $\{\bar{b}_t^i\}_{i=0}^4$. In Band Control, the power allocation is exactly the added $\{\bar{p}_t^i\}_{i=0}^4$.

D. Transfer DDPG Output Action to Real Action

In this subsection, we discuss how to transfer DDPG output action to real action in proposed solutions. The UAV's positions have been discretized, therefore, its 3D flight actions are also discrete. The power and bandwidth allocation actions are continuous. DDPG only control continuous actions, so we should configure an action space to handle both discrete actions and continuous actions together. Finally, the neural networks of the actor and critic are set based on the configure.

Firstly, we discuss the action subspaces: the UAV's horizontal flight and vertical flight, power allocation, and bandwidth allocation. 1) The UAV's horizontal flight and vertical flight constitute the discrete actions. The dimension of the UAV's horizontal and vertical flight actions is ϕ_h and ϕ_v , respectively. ϕ_h is exactly the number of the UAV's horizontal flight actions, and ϕ_v is exactly the number of the UAV's vertical flight actions. The chosen horizontal and vertical flight actions are denoted by a_t^h and a_t^v , respectively. We assume that the UAV's horizontal flight actions are put in front of vertical flight actions in the DDPG output action a_t . Let $a_t^i \in [-1, 1]$ be the i th DDPG output action in time slot t . 2) The dimension of the power allocation among all blocks ϕ_p is the number of blocks. 3) The dimension of bandwidth allocation among all blocks ϕ_b is also the number of blocks.

The chosen actions for the UAV's horizontal and vertical flight are formulated by (23) and (24), respectively. The real power and bandwidth allocations obtained from DDPG output action $(\{a_t^i\}_{i=0}^{\phi_h-1}, \{a_t^i\}_{i=\phi_h}^{\phi_h+\phi_v-1}, \{\bar{p}_t^i\}_{i=0}^4, \{\bar{b}_t^i\}_{i=0}^4)$, added equal power allocation $(\{\bar{p}_t^i\}_{i=0}^4)$, and added equal bandwidth allocation $(\{\bar{b}_t^i\}_{i=0}^4)$ are shown in (25) and (26), respectively. Note that the number of channels allocated to vehicles in each block i in time slot t from DDPG output and added equal bandwidth allocation is $\left\lfloor \frac{\bar{b}_t^i+1}{\sum_{j=0}^4(\bar{b}_t^j+1)} \kappa \right\rfloor$ and $\left\lfloor \frac{\bar{b}_t^i}{\sum_{j=0}^4 \bar{b}_t^j \kappa} \right\rfloor$, respectively, both of which are integers.

$$a_t^h = \text{argmax}\{a_t^i\}_{i=0}^{\phi_h-1}, \quad (23)$$

$$a_t^v = \text{argmax}\{a_t^i\}_{i=\phi_h}^{\phi_h+\phi_v-1} - \phi_h - \frac{\phi_v - 1}{2}, \quad (24)$$

$$p_t^i = \begin{cases} \frac{\bar{p}_t^i+1}{\sum_{j=0}^4(\bar{p}_t^j+1)} P, & \text{if Power/Joint Control,} \\ \frac{\bar{p}_t^i}{\sum_{j=0}^4 \bar{p}_t^j} P, & \text{if Band Control,} \end{cases} \quad (25)$$

$$b_t^i = \begin{cases} \left\lfloor \frac{\bar{b}_t^i+1}{\sum_{j=0}^4(\bar{b}_t^j+1)} \kappa \right\rfloor \frac{B}{\kappa}, & \text{if Band/Joint Control,} \\ \left\lfloor \frac{\bar{b}_t^i}{\sum_{j=0}^4 \bar{b}_t^j \kappa} \right\rfloor \frac{B}{\kappa}, & \text{if Power Control} \end{cases} \quad (26)$$

where $\bar{p}_t^j \in [-1, 1]$ and $\bar{b}_t^j \in [-1, 1]$ are the DDPG output actions for power and bandwidth allocation in block j in time slot t .

Secondly, we discuss the action space of three solutions. In Power Control, DDPG only controls the UAV's 3D flight and power allocation, therefore, the dimension of actions is $\phi_h + \phi_v + \phi_p$. In Band Control, DDPG only controls the UAV's 3D flight and bandwidth allocation, therefore, the dimension of actions is $\phi_h + \phi_v + \phi_b$. In Joint Control, DDPG controls the UAV's 3D flight, power allocation and bandwidth allocation, therefore, the dimension of actions is $\phi_h + \phi_v + \phi_p + \phi_b$. The dimension of actions ϕ in three solutions is formulated as

$$\phi = \begin{cases} \phi_h + \phi_v + \phi_p, & \text{if Power Control,} \\ \phi_h + \phi_v + \phi_b, & \text{if Band Control,} \\ \phi_h + \phi_v + \phi_p + \phi_b, & \text{if Joint Control.} \end{cases} \quad (27)$$

Thirdly, we discuss the neural networks of the actor and critic, which are set based on the configure of the action space. A the neural network consists of input layer, fully-connected layer, and output layer. The number of fully-connected layer in actor and critic both is set to 8, and the dimension of the output space is set to 10ϕ , which is generally set larger than the dimension of output.

V. PERFORMANCE EVALUATION

For a one-way-two-flow road intersection in Fig. 2, we present the optimality verification of deep reinforcement learning algorithms. Then, we study a more realistic road intersection as shown in Fig. 7, and present our simulation results.

Our simulations are executed on a server with Linux OS, 200 GB memory, two Intel(R) Xeon(R) Gold 5118 CPUs@2.30 GHz, a Tesla V100-PCIE GPU and four RTX 2080 Ti GPUs.

The implementation of Algorithm 1 includes two parts: using the DDPG algorithm in TensorFlow [37], and building the environment (including traffic and communication models) for our scenarios.

A. Optimality Verification of Deep Reinforcement Learning

Theoretically, it is well-known that deep reinforcement learning algorithms (including DDPG algorithms) solve MDP problems and achieve the optimal results with much less memory and computation resources. We provide the optimality verification of DDPG-based algorithms in Alg. 1 in a one-way-two-flow road intersection in Fig. 2. The reasons are as follows: (i) the MDP problem in such a simplified scenario is explicitly defined and the theoretically optimal policy can be obtained using the Python MDP Toolbox [38]; and (ii) this optimality verification process also serves a good code debugging process before we apply the DDPG algorithm

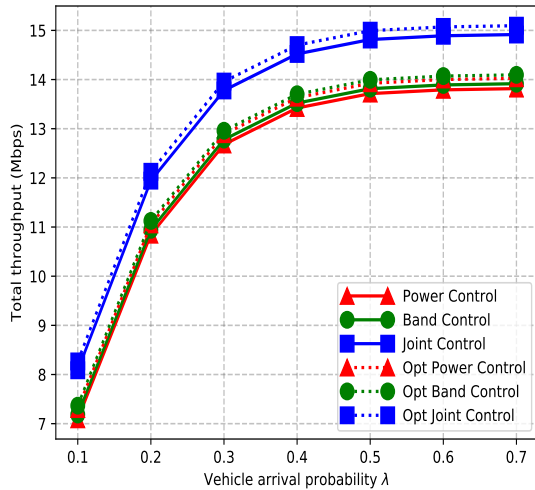


Fig. 6. Total throughput vs. vehicle arrival probability λ in optimality verification.

in TensorFlow [37] to the more realistic road intersection scenario in Fig. 7.

The assumptions and settings of the simplified scenario in Fig. 2 are as follows. To keep the state space small for verification purpose, we assume all the communication links are LoS, and the UAV's height is fixed as 50, so that the UAV can only adjusts its horizontal flight control. The traffic light state is assumed to have two values (red or green). The power and bandwidth allocation actions for each block i have three values, and the total number of channels κ is 256, and the vehicle arrival probabilities for block 1 and 2 are the same and are in the range $0.1 \sim 0.7$, and the discount factor γ is 0.9.

The result of DDPG-based algorithms matches that of the policy iteration algorithm using Python MDP Toolbox [38] (serving as the optimal policy). The total throughput obtained by the policy iteration algorithm and DDPG-based algorithms are shown as dashed lines and solid lines in Fig. 6. Therefore, DDPG-based algorithms achieve near optimal policies. We see that, the total throughput in Joint Control is the largest, which is much higher than Power Control and Band Control. This is in consistent with our believes that the joint control of power and bandwidth allocation will be better than the control of either of both. The performance of Power Control is almost the same as Band Control, since the power and bandwidth almost have the same effects on communication performance. The throughput increases with the increasing of vehicle arrival probability λ in all algorithms, and it saturates when $\lambda \geq 0.6$ due to traffic congestion.

B. More Realistic Traffic Model

We consider a more realistic road intersection model in Fig. 7. There are totally 33 blocks with four entrances (block 26, 28, 30, and 32), and four exits (block 25, 27, 29, and 31). Vehicles in block $i \in \{2, 4, 6, 8\}$ go straight, turn left, turn right with the probabilities g_i^s , g_i^l , and g_i^r , such that

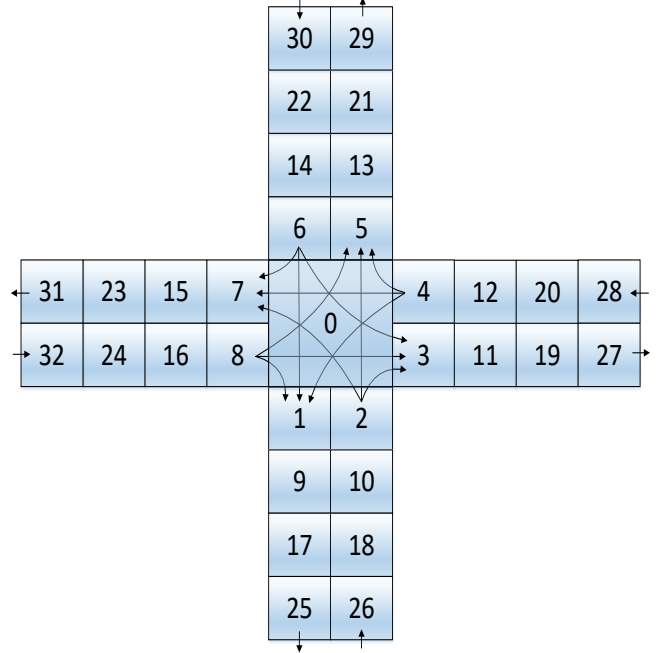


Fig. 7. Realistic road intersection model.

$g_i^s + g_i^l + g_i^r = 1$. We assume vehicles can turn right when the traffic light is green. We assume $\{n_j\}_{j \in \{26, 28, 30, 32\}}$ follows a binomial distribution with the same parameter λ . The blocks' distance is easily calculated as follows: $D(1, 2) = \hat{d}$, and $D(1, 6) = 3\hat{d}$, where $D(i, j)$ is the Euclidean distance from block i to block j , and \hat{d} is the length of a block.

The UAV's flight movements are as follows. We assume that the UAV's block is $0 \sim 8$ since the number of vehicles in the intersection block 0 is generally the largest and the UAV will not move to the block far from the intersection block. Moreover, within a time slot we assume that the UAV can stay or only move to its adjacent blocks.

The parameter settings are summarized in Table II. In the simulations, there are three types of parameters: DDPG algorithm parameters, communication parameters, and UAV/vehicle parameters.

First, we describe the DDPG algorithm parameters. The number of episodes is 256, and the number of timesteps in an episode is 256, so the number of total time slots is 65,536. The experience replay buffer capacity is 10,000, and the learning rate of target networks τ is 0.01. The learning rate of the actor and critic is 0.001 and 0.002, respectively. The discount factor γ is $0.4 \sim 0.9$, and the mini-batch size M is 512.

Secondly, we describe communication parameters. α_1 and α_2 are set to 9.6 and 0.28, which are common values in urban areas [39]. β_1 is 3, and β_2 is 0.01, which are widely used in path loss modeling. The duration of a time slot is set to 6 seconds, and the number of occupied red or green traffic light N is 10, i.e., 60 seconds constitute a red/green duration, which is commonly seen in cities and can ensure that the vehicles in blocks can get the next block in a time slot. The white power spectral density σ^2 is set to -130 dBm/Hz. The total UAV transmission power P is set to 1 ~ 6 W in consideration of the

TABLE II
VALUES OF PARAMETERS IN SIMULATION SETTINGS

α_1	α_2	β_1	β_2	σ^2	\hat{d}
9.6	0.28	3	0.01	-130 dBm/Hz	3
P	B	N	γ	z^0	z^{38}
$1 \sim 6$	$0.5 \sim 1$ MHz	10	$0.4 \sim 0.9$	10	200
K	λ	g_i^s	g_i^l	g_i^r	κ
39	$0.1 \sim 0.7$	0.4	0.3	0.3	256
τ	M				
0.01	512				

limited communication ability. The total bandwidth allocated for vehicles B is $0.5 \sim 1$ MHz.

Thirdly, we describe UAV/vehicle parameters. The maximum vertical distance that the UAV can move in a time slot is set to 5 meters considering of its speed. The number of discretized distance K of the UAV's height is 39, and the minimum and maximum height of the UAV (z^0 and z^{38}) is 10 meters and 200 meters. Therefore, the UAV has three vertical flight actions: -1, 0, and 1, which denote flying down 5 meters, staying at the current height, and flying up 5 meters. λ is set to $0.1 \sim 0.7$. The length of a road block \hat{d} is set to 3 meters. The probability of a vehicle going straight, turning left, and turning right g_i^s , g_i^l , and g_i^r , is set to 0.4, 0.3, and 0.3, respectively, and each of them is assumed to be the same in block 2, 4, 6, and 8. The total number of channels κ is 256.

C. Baseline Schemes

We compare with two baseline schemes. Generally, the equal transmission power and bandwidth allocation is common in communication systems for fairness.

The first baseline scheme is Cycle, i.e., the UAV cycles anticlockwise at a fixed height (e.g., 150 meters), and the UAV allocates the transmission power and bandwidth equally to each vehicle in each time slot. The UAV moves along the fixed trajectory periodically, without considering the vehicle flows.

The second baseline scheme is Greedy, i.e., at a fixed height (e.g., 150 meters), the UAV greedily moves to the block with the largest number of vehicles. If a nonadjacent block has the largest number of vehicles, the UAV has to move to block 0 and then move to that block. The UAV also allocates the transmission power and the bandwidth equally to each vehicle in each time slot. The UAV tries to serve the road segment with the largest number of vehicles by moving nearer to them.

D. Simulation Results

Next, we first show the convergence of loss functions, and then show the throughput vs. discount factor, the total transmission power, the total bandwidth and the vehicle arrival probability.

The convergence of loss functions in Power Control, Band Control, and Joint Control indicates that the neural network is well-trained. It is shown in Fig. 8 when $P = 6$, $B = 1$ MHz, $\lambda = 0.5$ and $\gamma = 0.9$ during time slot 12,000 \sim 13,000. The first 12,000 time slots are not shown since during the 0 \sim 12,000, the experience replay buffer has not achieved its

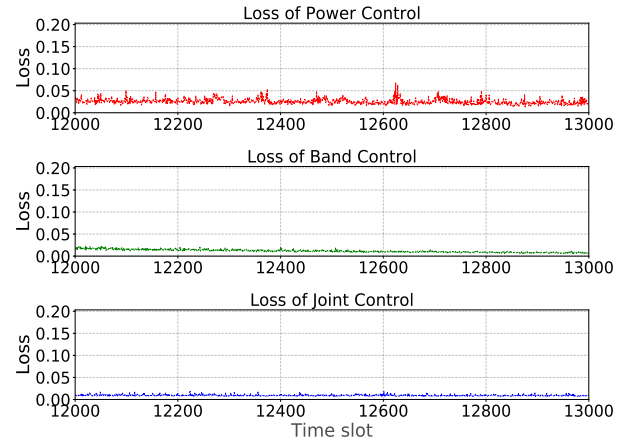


Fig. 8. Convergence of loss functions in Power Control, Band Control, and Joint Control.

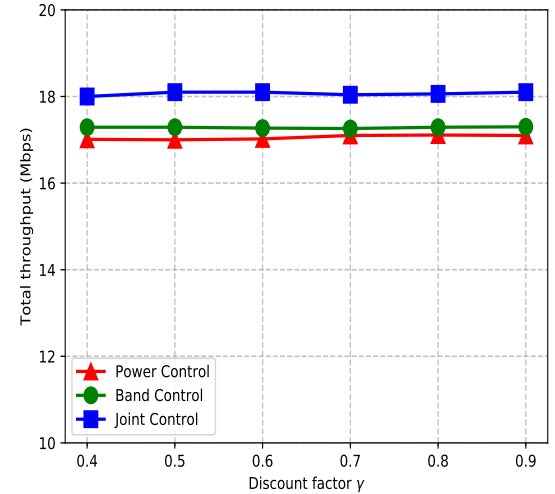
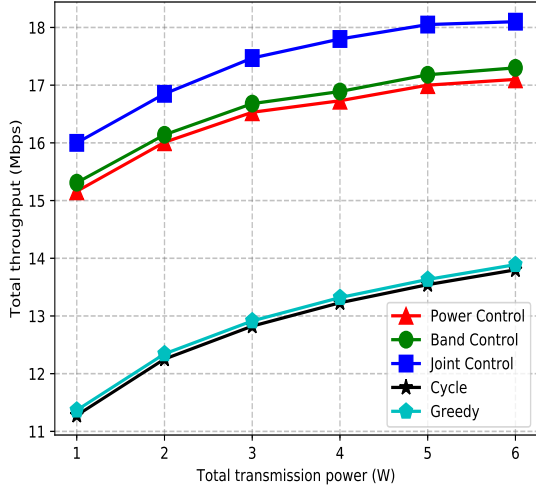
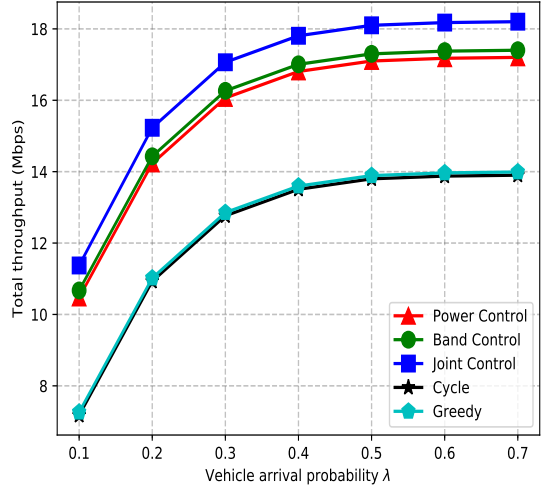
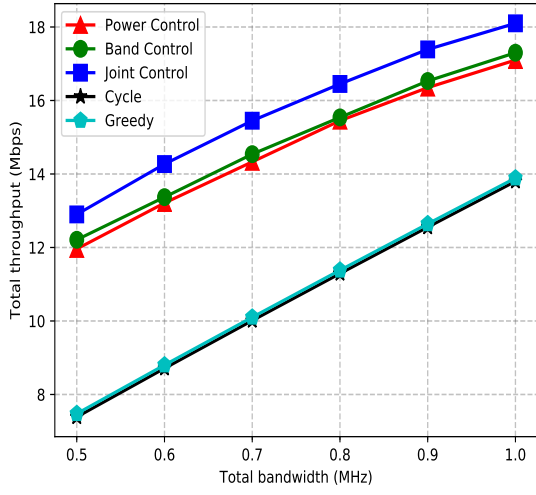


Fig. 9. Throughput vs. discount factor γ .

capacity, and from 10,000 \sim 12,000, the fluctuation is large after the R_b is full. We see that, the loss functions in three algorithms converge after 12,000 time slots.

The throughput vs. discount factor γ is drawn in Fig. 9 when $P = 6$, $B = 1$ MHz, and $\lambda = 0.5$. We can see that, when γ changes, the throughput of three algorithms is steady; and Joint Control achieves higher total throughput, comparing with Power Control and Band Control, respectively.

The throughput vs. the total transmission power ($P = 1 \sim 6$) and the total bandwidth ($B = 0.5 \sim 1$ MHz) are shown by Fig. 10 and Fig. 11, where we set $\lambda = 0.5$ and $\gamma = 0.9$. We see that DDPG achieves the best performance for different transmission power and bandwidth budgets, respectively. Moreover, the total throughput of all algorithms increases when the total transmission power or bandwidth increases. Power Control and Band Control only adjust the transmission power or bandwidth, while Joint Control can jointly adjust both of them, so its performance is the best.

Fig. 10. Total throughput vs. the total transmission power ($B = 1$ MHz).Fig. 12. Total throughput vs. the vehicle arrival probability λ .Fig. 11. Total throughput vs. the total bandwidth ($P = 6$ W).

The total throughput of DDPG-based algorithms is improved greatly than that of Cycle and Greedy. The performance of Greedy is a little better than Cycle, since Greedy tries to get nearer to the block with the largest number of vehicles.

Total throughput vs. the vehicle arrival probability λ is shown in Fig. 12. Note that the road intersection has a capacity of 2 units, i.e., can serve at most two traffic flows, therefore, it cannot serve traffic flows where λ is high, e.g., $\lambda = 0.8$ and $\lambda = 0.9$. We see that, when λ increases, i.e., more vehicles arrive at the intersection, the total throughput increases. However, when λ gets higher, e.g., $\lambda = 0.6$, the total throughput saturates due to traffic congestion.

VI. DISCUSSION AND CONCLUSION

We studied a UAV-assisted vehicular network where the UAV acted as a relay to maximize the total throughput between

the UAV and vehicles. We focused on the downlink communication where the UAV could adjust its transmission power and bandwidth allocation under 3D flight. We formulated this problem as a MDP problem, explored the state transitions of UAV and vehicles under different actions, and then proposed three deep reinforcement learning schemes based on the DDPG algorithms. In a simplified scenario with small state space and action space, we verify the optimality of DDPG-based algorithms. Then, through extensive simulation results, we demonstrated the performance of the algorithms under a more realistic traffic scenario, comparing with two baseline schemes.

In the future, we will consider the scenario where multiple UAVs constitute a relay network to assist vehicular networks and study the coverage overlap/probability, relay selection, energy-aware communications, and UAV cooperative communication protocols.

REFERENCES

- [1] M. Chaqfeh, H. El-Sayed, and A. Lakas, "Efficient data dissemination for urban vehicular environments," *IEEE Transactions on Intelligent Transportation Systems (TITS)*, no. 99, pp. 1–11, 2018.
- [2] M. Zhu, X.-Y. Liu, F. Tang, M. Qiu, R. Shen, W. Shu, and M.-Y. Wu, "Public vehicles for future urban transportation," *IEEE Transactions on Intelligent Transportation Systems (TITS)*, vol. 17, no. 12, pp. 3344–3353, 2016.
- [3] M. Zhu, X.-Y. Liu, and X. Wang, "Joint transportation and charging scheduling in public vehicle systems - a game theoretic approach," *IEEE Transactions on Intelligent Transportation Systems (TITS)*, vol. 19, no. 8, pp. 2407–2419, 2018.
- [4] M. Zhu, X.-Y. Liu, and X. Wang, "An online ride-sharing path-planning strategy for public vehicle systems," *IEEE Transactions on Intelligent Transportation Systems (TITS)*, vol. 20, no. 2, pp. 616–627, 2019.
- [5] K. Li, C. Yuen, S. S. Kanhere, K. Hu, W. Zhang, F. Jiang, and X. Liu, "An experimental study for tracking crowd in smart cities," *IEEE Systems Journal*, 2018.
- [6] F. Cunha, L. Villas, A. Boukerche, G. Maia, A. Viana, R. A. Mini, and A. A. Loureiro, "Data communication in vanets: Protocols, applications and challenges," *Elsevier Ad Hoc Networks*, vol. 44, pp. 90–103, 2016.

[7] H. Sedjelmaci, S. M. Senouci, and N. Ansari, "Intrusion detection and ejection framework against lethal attacks in uav-aided networks: a bayesian game-theoretic methodology," *IEEE Transactions on Intelligent Transportation Systems (TITS)*, vol. 18, no. 5, pp. 1143–1153, 2017.

[8] "Paving the path to 5g: Optimizing commercial lte networks for drone communication (2018)."
<https://www.qualcomm.cn/videos/paving-path-5g-optimizing-commercial-lte-networks-drone-communication>.

[9] "Huawei signs mou with china mobile sichuan and fonair aviation to build cellular test networks for logistics drones (2018)."
<https://www.huawei.com/en/press-events/news/2018/3/MoU-ChinaMobile-FonairAviation-Logistics>.

[10] M. Alzenad, A. El-Keyi, F. Lagum, and H. Yanikomeroglu, "3-d placement of an unmanned aerial vehicle base station (uav-bs) for energy-efficient maximal coverage," *IEEE Wireless Communications Letters (WCL)*, vol. 6, no. 4, pp. 434–437, 2017.

[11] M. Giordani, M. Mezzavilla, S. Rangan, and M. Zorzi, "An efficient uplink multi-connectivity scheme for 5g mmwave control plane applications," *IEEE Transactions on Wireless Communications (TWC)*, 2018.

[12] Q. Yang and S.-J. Yoo, "Optimal uav path planning: Sensing data acquisition over iot sensor networks using multi-objective bio-inspired algorithms," *IEEE Access*, vol. 6, pp. 13671–13684, 2018.

[13] M. Garraffa, M. Bekhti, L. Létocart, N. Achir, and K. Boussetta, "Drones path planning for wsn data gathering: A column generation heuristic approach," in *IEEE Wireless Communications and Networking Conference (WCNC)*, pp. 1–6, 2018.

[14] C. H. Liu, Z. Chen, J. Tang, J. Xu, and C. Piao, "Energy-efficient uav control for effective and fair communication coverage: A deep reinforcement learning approach," *IEEE Journal on Selected Areas in Communications (JSAC)*, vol. 36, no. 9, pp. 2059–2070, 2018.

[15] H. Wang, G. Ding, F. Gao, J. Chen, J. Wang, and L. Wang, "Power control in uav-supported ultra dense networks: Communications, caching, and energy transfer," *IEEE Communications Magazine*, vol. 56, no. 6, pp. 28–34, 2018.

[16] S. Yan, M. Peng, and X. Cao, "A game theory approach for joint access selection and resource allocation in uav assisted iot communication networks," *IEEE Internet of Things Journal (IOTJ)*, 2018.

[17] Y. Wu, J. Xu, L. Qiu, and R. Zhang, "Capacity of uav-enabled multicast channel: Joint trajectory design and power allocation," in *IEEE International Conference on Communications (ICC)*, pp. 1–7, 2018.

[18] Y. Zeng, X. Xu, and R. Zhang, "Trajectory design for completion time minimization in uav-enabled multicasting," *IEEE Transactions on Wireless Communications (TWC)*, vol. 17, no. 4, pp. 2233–2246, 2018.

[19] S. Zhang, Y. Zeng, and R. Zhang, "Cellular-enabled uav communication: Trajectory optimization under connectivity constraint," in *IEEE International Conference on Communications (ICC)*, pp. 1–6, 2018.

[20] R. Fan, J. Cui, S. Jin, K. Yang, and J. An, "Optimal node placement and resource allocation for uav relaying network," *IEEE Communications Letters*, vol. 22, no. 4, pp. 808–811, 2018.

[21] U. Challita, W. Saad, and C. Bettstetter, "Deep reinforcement learning for interference-aware path planning of cellularconnected uavs," in *IEEE International Conference on Communications (ICC)*, 2018.

[22] X.-Y. Liu, Z. Ding, S. Borst, and A. Walid, "Deep reinforcement learning for intelligent transportation systems," in *NeurIPS Workshop on Machine Learning for Intelligent Transportation Systems*, 2018.

[23] A. Al-Hourani, S. Kandeepan, and S. Lardner, "Optimal lap altitude for maximum coverage," *IEEE Wireless Communications Letters (WCL)*, vol. 3, no. 6, pp. 569–572, 2014.

[24] M. Mozaffari, W. Saad, M. Bennis, and M. Debbah, "Unmanned aerial vehicle with underlaid device-to-device communications: Performance and tradeoffs," *IEEE Transactions on Wireless Communications (TWC)*, vol. 15, no. 6, pp. 3949–3963, 2016.

[25] D. Oehmann, A. Awada, I. Viering, M. Simsek, and G. P. Fettweis, "Sinr model with best server association for high availability studies of wireless networks," *IEEE Wireless Communications Letters (WCL)*, vol. 5, no. 1, pp. 60–63, 2015.

[26] V. Vahidi, E. Saberinia, and B. T. Morris, "Ofdm performance assessment for traffic surveillance in drone small cells," *IEEE Transactions on Intelligent Transportation Systems (TITS)*, 2018.

[27] P. Ramezani and A. Jamalipour, "Throughput maximization in dual-hop wireless powered communication networks," *IEEE Transactions on Vehicular Technology (TVT)*, vol. 66, no. 10, pp. 9304–9312, 2017.

[28] R. S. Sutton and A. G. Barto, *Reinforcement learning: An introduction*. MIT press, 2018.

[29] H. Van Hasselt, A. Guez, and D. Silver, "Deep reinforcement learning with double q-learning," in *AAAI Conference on Artificial Intelligence*, 2016.

[30] T. P. Lillicrap, J. J. Hunt, A. Pritzel, N. Heess, T. Erez, Y. Tassa, D. Silver, and D. Wierstra, "Continuous control with deep reinforcement learning," in *International Conference on Learning Representations (ICLR)*, 2016.

[31] D. Silver, J. Schrittwieser, K. Simonyan, I. Antonoglou, A. Huang, A. Guez, T. Hubert, L. Baker, M. Lai, A. Bolton, et al., "Mastering the game of go without human knowledge," *Nature*, vol. 550, no. 7676, p. 354, 2017.

[32] V. Mnih, K. Kavukcuoglu, D. Silver, A. Graves, I. Antonoglou, D. Wierstra, and M. Riedmiller, "Playing atari with deep reinforcement learning," *arXiv preprint arXiv:1312.5602*, 2013.

[33] P.-W. Chou, D. Maturana, and S. Scherer, "Improving stochastic policy gradients in continuous control with deep reinforcement learning using the beta distribution," in *International Conference on Machine Learning (ICML)*, pp. 834–843, 2017.

[34] A. Daniely, "Sgd learns the conjugate kernel class of the network," in *Advances in Neural Information Processing Systems (NIPS)*, pp. 2422–2430, 2017.

[35] D. P. Kingma and J. Ba, "Adam: A method for stochastic optimization," *arXiv preprint arXiv:1412.6980*, 2014.

[36] I. Bello, B. Zoph, V. Vasudevan, and Q. V. Le, "Neural optimizer search with reinforcement learning," in *Proceedings of the International Conference on Machine Learning-Volume*, pp. 459–468, 2017.

[37] M. Abadi, P. Barham, J. Chen, Z. Chen, A. Davis, J. Dean, M. Devin, S. Ghemawat, G. Irving, M. Isard, et al., "Tensorflow: A system for large-scale machine learning," in *USENIX Symposium on Operating Systems Design and Implementation (OSDI)*, pp. 265–283, 2016.

[38] "Python markov decision process (mdp) toolbox (2019)."
<https://pymdptoolbox.readthedocs.io/en/latest/api/mdptoolbox.html>.

[39] M. Mozaffari, W. Saad, M. Bennis, and M. Debbah, "Drone small cells in the clouds: Design, deployment and performance analysis," in *IEEE Global Communications Conference (GLOBECOM)*, pp. 1–6, 2015.



Ming Zhu received the Ph.D. degree in Computer Science and Engineering in Shanghai Jiao Tong University, Shanghai, China. He is now a Post-Doctoral Researcher and an Assistant Researcher in Shenzhen Institutes of Advanced Technology, Chinese Academy of Sciences, Shenzhen, China.

His research interests are in the area of big data, artificial intelligence, intelligent transportation systems, smart cities, and wireless communications.



Xiao-Yang Liu received the B.Eng. degree in Computer Science from Huazhong University of Science and Technology, and the PhD degree in the Department of Computer Science and Engineer, Shanghai Jiao Tong University, China. He is currently a PhD in the Department of Electrical Engineering, Columbia University.

His research interests include tensor theory, deep learning, non-convex optimization, big data analysis and IoT applications.



Xiaodong Wang (S'98-M'98-SM'04-F'08) received the Ph.D. degree in electrical engineering from Princeton University. He is currently a Professor of electrical engineering with Columbia University, New York NY, USA. His research interests fall in the general areas of computing, signal processing, and communications. He has authored extensively in these areas. He has authored the book entitled *Wireless Communication Systems: Advanced Techniques for Signal Reception*, (Prentice Hall, 2003).

His current research interests include wireless communications, statistical signal processing, and genomic signal processing. He has served as an Associate Editor of the *IEEE TRANSACTIONS ON COMMUNICATIONS*, *IEEE TRANSACTIONS ON WIRELESS COMMUNICATIONS*, *IEEE TRANSACTIONS ON SIGNAL PROCESSING*, and *IEEE TRANSACTIONS ON INFORMATION THEORY*. He is an ISI Highly Cited Author. He received the 1999 NSF CAREER Award, the 2001 IEEE Communications Society and Information Theory Society Joint Paper Award, and the 2011 IEEE Communication Society Award for Outstanding Paper on New Communication Topics.